

Physics-Informed Diffusion Models for Vehicle Speed Trajectory Generation

Vadim Sokolov

Farnaz Behnia

Dominik Karbowski

George Mason University

George Mason University

Argonne National Laboratory

Abstract—Synthetic vehicle speed trajectory generation is essential for evaluating vehicle control algorithms and connected vehicle technologies. Traditional Markov chain approaches suffer from discretization artifacts and limited expressiveness. This paper proposes a physics-informed diffusion framework for conditional micro-trip synthesis, combining a dual-channel speed-acceleration representation with soft physics constraints that resolve optimization conflicts inherent to hard-constraint formulations. We compare a 1D U-Net architecture against a transformer-based Conditional Score-based Diffusion Imputation (CSDI) model using 6,367 GPS-derived micro-trips. CSDI achieves superior distribution matching (Wasserstein distance 0.30 for speed, 0.026 for acceleration), strong indistinguishability from real data (discriminative score 0.49), and validated utility for downstream energy assessment tasks. The methodology enables scalable generation of realistic driving profiles for intelligent transportation systems (ITS) applications without costly field data collection.

I. INTRODUCTION

Accurate modeling of vehicle speed trajectories is fundamental to numerous applications in intelligent transportation systems (ITS), including energy consumption assessment (Karbowski, Sokolov, and Rousseau 2015; Karbowski et al. 2016; Karbowski, Sokolov, and Jongryeol 2016), route optimization (Moawad et al. 2021), traffic simulation (Auld et al. 2013; Auld, Hope, et al. 2016), and predictive control of autonomous vehicles (Dauner et al. 2023). The ability to generate synthetic speed profiles that faithfully reproduce the statistical and physical characteristics of real-world driving behavior enables scalable evaluation of transportation policies, vehicle technologies, and traffic management strategies without the prohibitive cost of extensive field data collection.

Traditional approaches to synthetic trajectory generation have relied on Markov chain models (Karbowski et al., n.d., 2016), which discretize the speed state space and model transitions between consecutive states. While computationally efficient and interpretable, these methods face fundamental limitations: rigid discretization loses fine-grained dynamics, the Markov assumption ignores long-range temporal dependencies, and incorporating physics-based constraints or conditional controls (e.g., powertrain type, road conditions) requires ad-hoc engineering. More

recent efforts have explored deep generative models, including generative adversarial networks (GANs) (Behnia, Karbowski, and Sokolov 2023; Yoon, Jarrett, and van der Schaar 2019) and normalizing flows (Papamakarios et al. 2019), with mixed success due to training instability, mode collapse, and difficulty enforcing hard boundary constraints.

This paper introduces an application of denoising diffusion probabilistic models (DDPMs) (Ho, Jain, and Abbeel 2020) to the problem of conditional vehicle speed trajectory synthesis. Diffusion models have emerged as an effective class of generative models, demonstrating strong performance in image generation, audio synthesis, and recently, time series forecasting (Ansari et al. 2025). Their key advantages include stable training dynamics, the ability to naturally model complex multi-modal distributions, and relevant for this application, a principled mechanism for enforcing constraints through inpainting during the reverse diffusion process. Unlike prior work on diffusion-based trajectory generation for autonomous driving (Feng et al. 2023; Suo et al. 2021), which focuses on spatial path planning in multi-agent scenarios, we target univariate speed profiles for energy assessment applications, requiring strict enforcement of micro-trip boundaries (zero initial and final speeds) and precise control over aggregate statistics (average speed, duration).

We compare two diffusion-based architectures: a standard 1D U-Net diffusion model and a Conditional Score-based Diffusion Imputation (CSDI) model (Tashiro et al. 2021) adapted from time series imputation. Both models are conditioned on trip characteristics (target average speed, duration) and trained on 6,367 micro-trip observations from the 2007 Chicago Metropolitan Agency for Planning (CMAP) Regional Household Travel Survey. Our investigation systematically explores the evolution of these models through multiple design iterations, documenting the failures of hard-constraint physics penalties in standard diffusion and the successful integration of soft physics constraints in CSDI. We benchmark these approaches against traditional Markov chain baselines and analyze the failure modes of alternative deep generative methods (DopelGANger, SDV) to provide guidance for practitioners.

The practical utility of high-fidelity synthetic trajectory generation spans several key areas of intelligent transportation systems. For energy assessment, synthetic trajectories enable evaluation of electric vehicle range, charging infrastructure requirements, and fleet electrification strategies across diverse driving scenarios without costly field trials (Chen et al. 2016; X. Huang et al. 2020). Traffic microsimulation platforms like POLARIS (Auld, Hope, et al. 2016) require realistic speed profiles to accurately model emissions, fuel consumption, and network-level energy impacts. Connected and autonomous vehicle testing demands diverse, physically plausible trajectories for validating perception, planning, and control systems (Mozaffari et al. 2020), as well as generating representative safety-critical scenarios (Wu et al. 2025). By demonstrating both distributional fidelity (via Wasserstein metrics) and downstream utility (via TSTR), this work provides a validated methodology for generating synthetic driving data that directly supports ITS energy management, simulation-based policy analysis, and intelligent vehicle development.

The principal contributions of this work are:

1. The first application of diffusion models specifically to vehicle speed micro-trip generation for transportation energy assessment, demonstrating superior distribution matching compared to Markov chains and GANs.
2. The first successful integration of kinematic physics constraints into transformer-based diffusion for transportation, combining direct speed and acceleration channels with physics-based training objectives to effectively bridge the gap between deep generative modeling and kinematic consistency.
3. Documentation of the complete model development lifecycle, including failures (hard-constraint diffusion, DoppelGANger, SDV), providing insights into why certain approaches fail and how to avoid common pitfalls in generative modeling for transportation applications.
4. A rigorous evaluation framework encompassing distributional fidelity (Wasserstein distance, MMD), kinematic validity (smoothness metrics, boundary violations), and utility (discriminative score, TSTR), establishing best practices for assessing synthetic trajectory quality.
5. Open-source implementation and reproducibility package at <https://github.com/VadimSokolov/diffusion-trajectory-generation>, including complete training code, pretrained model weights, preprocessed data, and figure generation scripts enabling full reproduction of all results.

The remainder of this paper is organized as follows: Section II reviews related work in vehicle trajectory generation, deep generative models for time series, and diffusion

models. Section III describes the CMAP dataset, preprocessing, and clustering analysis. Section IV presents the methodology, including problem formulation, the Markov chain baseline, and detailed descriptions of the diffusion and CSDI architectures along with their evolution through multiple design iterations. Section V reports quantitative and qualitative results, comparing all approaches and documenting failure modes. Section VI discusses implications for practice, limitations, and future research directions.

II. RELATED WORK

The problem of generating realistic vehicle trajectories has been approached from multiple perspectives in the transportation literature. Early work relied on parametric models and Markov processes to capture driving patterns (Karbowski et al., n.d., 2016), where speed transitions are modeled as discrete-state stochastic processes. Karbowski et al. developed Markov chain models for trip prediction in energy-efficient vehicle routing, demonstrating that second-order Markov models can capture speed-acceleration dependencies (Karbowski, Sokolov, and Jongryeol 2016). While interpretable and computationally efficient, these approaches are limited by their memoryless nature and inability to model long-range temporal dependencies inherent in driving behavior.

Agent-based traffic simulation platforms such as POLARIS (Sokolov, Auld, and Hope 2012; Auld et al. 2013; Auld, Hope, et al. 2016) have incorporated microsimulation of individual vehicle movements to assess regional transportation policies. These systems combine activity-based demand models with network assignment, requiring realistic speed profiles as inputs (Auld, Karbowski, et al. 2016). Moawad et al. proposed neural recommender systems for real-time route assignment considering energy consumption, highlighting the need for fast generation of representative speed trajectories conditioned on route characteristics (Moawad et al. 2021).

More recently, Behnia et al. explored deep generative models for vehicle speed trajectories, comparing variational autoencoders (VAEs), GANs, and normalizing flows (Behnia, Karbowski, and Sokolov 2023). Their analysis demonstrated that GANs achieved the best distribution matching but suffered from training instability and mode collapse, particularly for diverse driving regimes. This work established important evaluation metrics for trajectory generation but did not explore diffusion models, which have since emerged as a more stable alternative to GANs.

Adjacent to single-vehicle speed generation is the rapidly growing literature on multi-agent trajectory prediction and scenario generation for autonomous vehicle testing. TrafficGen (Feng et al. 2023) and ScenarioNet (Li et al. 2023) introduced learning-based frameworks for generating diverse, realistic traffic scenarios from large-scale

driving datasets. TrafficSim (Suo et al. 2021) proposed a multi-agent behavioral model learning to simulate realistic interactions among vehicles.

These works differ fundamentally from our focus: they generate spatial trajectories (x, y coordinates over time) for multiple interacting agents in 2D road networks, whereas we target univariate speed profiles for isolated micro-trips. The former requires modeling complex spatial interactions and collision avoidance; the latter emphasizes matching kinematic distributions and enforcing strict boundary conditions for energy assessment. Nevertheless, recent applications of diffusion models to autonomous driving trajectory planning (Liao et al. 2024) and controllable motion generation (Lan et al. 2025) demonstrate the potential of this generative modeling paradigm for transportation applications.

The application of deep generative models to sequential data has evolved rapidly. TimeGAN (Yoon, Jarrett, and van der Schaar 2019) extended GANs to time series by combining unsupervised adversarial learning with supervised stepwise prediction, improving temporal coherence. DoppelGANger addressed the challenge of generating mixed-type time series with both temporal features and static attributes through a dual-stage generation process. However, both methods remain susceptible to mode collapse and require careful architectural tuning to enforce constraints.

Autoregressive models, including probabilistic variants implemented in the Synthetic Data Vault (SDV), represent another popular approach. The PARSynthesizer uses probabilistic autoregression to sequentially generate time steps conditioned on previous values. While simple to implement, these models suffer from exposure bias—errors accumulate over long sequences—and struggle with capturing diverse multi-modal distributions without explicit diversity mechanisms.

Foundation models for time series have recently emerged as zero-shot alternatives. Chronos (Ansari et al. 2025) adapts transformer language model architectures to probabilistic forecasting by tokenizing time series and training on diverse datasets. While showing promise for forecasting tasks, these models lack fine-grained control over generation and have not been extensively evaluated for constrained trajectory synthesis.

Denoising diffusion probabilistic models (DDPMs) (Ho, Jain, and Abbeel 2020) define a forward process that gradually corrupts data with Gaussian noise and learn a reverse process to denoise random samples into data. Unlike GANs, diffusion models optimize a tractable variational lower bound, resulting in stable training and high sample quality. Score-based generative models (Y. Song et al. 2020) provide an equivalent formulation by learning

the gradient of the data log-density (score function) and using Langevin dynamics for sampling.

The application of diffusion models to time series has largely focused on forecasting and imputation. CSDI (Conditional Score-based Diffusion for Imputation) (Tashiro et al. 2021) introduced a transformer-based diffusion architecture for missing value imputation in multivariate time series, demonstrating superior performance to autoregressive and GAN-based methods. The key innovation is self-attention’s ability to capture long-range dependencies while the diffusion framework handles uncertainty. We adapt this architecture for conditional generation by treating the entire trajectory as “missing” conditioned on aggregate trip statistics. Recent extensions in the ITS domain have combined diffusion with GANs for trajectory reconstruction (Qian et al. 2025) and proposed interpretable causal diffusion networks for speed prediction (Rong et al. 2025).

TimeGrad (Rasul et al. 2021) introduced autoregressive denoising diffusion for probabilistic time series forecasting, demonstrating strong performance on multivariate prediction tasks. SSSD (Alcaraz and Strothoff 2022) combined structured state-space models with diffusion for imputation and forecasting. TimeWeaver and Diffusion-TS have further extended diffusion models to multivariate time series synthesis. However, these methods do not address the specific challenges of vehicle trajectory generation: strict boundary constraints (zero start/end speeds), physics-based plausibility (acceleration limits, smoothness), and fine-grained conditional control (vehicle type, road conditions). While deep learning has been extensively applied to trajectory prediction in ITS (Schultz and Sokolov 2018; Mozaffari et al. 2020; Zhao et al. 2019; Altché and de La Fortelle 2017; Y. Huang et al. 2022), generation of complete speed profiles for energy assessment remains underexplored. Multi-agent diffusion models have also been explored for traffic flow prediction (Adam et al. 2025).

To our knowledge, this work is the first to apply diffusion models specifically to vehicle speed micro-trip generation for energy assessment, systematically comparing U-Net and transformer-based architectures and documenting the integration of physics-informed constraints.

III. DATA

The data for this study originate from the 2007 Chicago Metropolitan Agency for Planning (CMAP) Regional Household Travel Survey, conducted by NuStats for CMAP, an 11-county region, encompassing dense urban (Chicago), suburban, and rural environments. This geographic diversity ensures representation of varied driving conditions, road types, and traffic patterns.

The survey employed a dual-frame sampling strategy combining Random Digit Dialing (RDD) and address-based

sampling to reach over 3.2 million households. Data collection utilized Computer-Assisted Telephone Interview (CATI), mail questionnaires, and follow-up telephone interviews, achieving an overall response rate of 10 percent (19 percent recruitment rate, 55 percent retrieval rate) (Chicago Metropolitan Agency for Planning 2008). A subset of participating households contributed GPS-based trip-level data, which forms the basis of our analysis.

The dataset captures passenger vehicle movements (cars, SUVs, vans, pickup trucks) used for personal travel. Heavy-duty commercial vehicles and fleet operations are excluded. Road type coverage includes Interstate highways and expressways, major arterials connecting economic centers, and local urban and suburban roads. No filtering by road type was applied during collection; GPS traces reflect the natural distribution of household travel patterns.

A. Exploratory Data Analysis

Following preprocessing to extract individual micro-trips (continuous speed profiles beginning and ending at zero velocity), our dataset comprises 6,367 observations sampled at 1 Hz. Table I summarizes key distributional statistics.

Table I: Dataset Summary Statistics

Attribute	Min	Max	Mean	Median
Duration (s)	34	12,841	304	187
Duration (min)	0.57	214	5.06	3.12
Distance (m)	257	393,070	5,884	3,076
Distance (km)	0.26	393	5.88	3.08
Avg Speed (m/s)	5.18	31.57	16.92	16.45
Avg Speed (km/h)	18.63	113.66	60.92	59.21

The dataset exhibits substantial variation in trip characteristics, with durations ranging from half a minute to over three hours and distances spanning two orders of magnitude. Average speeds vary from slow urban crawl ($5 \text{ m/s} \approx 18 \text{ km/h}$) to highway cruising ($32 \text{ m/s} \approx 115 \text{ km/h}$), reflecting the diversity of driving contexts in the metropolitan area.

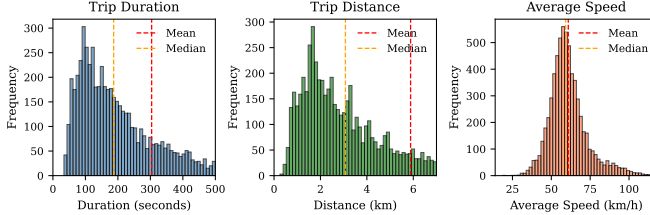


Figure 1: Data distributions for trip duration, distance, and average speed. Histograms show the empirical distributions from 6,367 micro-trips with mean (red dashed) and median (orange dashed) markers. The distributions exhibit substantial heterogeneity, reflecting diverse driving contexts from urban congestion to highway cruising.

To characterize the heterogeneity of driving patterns in the dataset, we performed K-means clustering ($K=4$) on

extracted features from each trajectory. Clustering serves two purposes: (1) understanding the data structure to inform model design, and (2) enabling stratified evaluation to ensure generated trajectories cover all driving regimes.

Feature Extraction: For each micro-trip, we computed:

- Average speed (\bar{v}) and maximum speed (v_{max})
- Speed standard deviation
- Idle time ratio (fraction of time at $v < 0.5 \text{ m/s}$)
- Stops per kilometer (number of near-zero speed events per unit distance)
- Acceleration noise (standard deviation of acceleration)

Clustering Results: The algorithm identified four distinct driving regimes, described in Table II:

Table II: Cluster Characteristics

Cluster Label	Count	Avg Speed (m/s)	Max Speed (m/s)	Stops/km	Idle Ratio (%)	
0	Arterial/Suburban	2,224	15.6	22.6	0.59	2.0
1	Highway/Interstate	1,020	22.2	30.8	0.12	0.5
2	Congested/City	636	13.9	21.8	1.29	4.4
3	Free-flow Arterial	2,487	16.7	22.7	0.28	1.0

Cluster 1 (Highway/Interstate) exhibits the highest average and maximum speeds with minimal stops and idle time, characteristic of uninterrupted highway travel. Cluster 2 (Congested/City) shows the opposite profile: low speeds, frequent stops (1.29 per km), and high idle time (4.4 percent), typical of stop-and-go urban driving. Clusters 0 and 3 represent intermediate arterial road conditions, with Cluster 3 having somewhat higher speeds and fewer stops, suggesting less congested arterial travel.

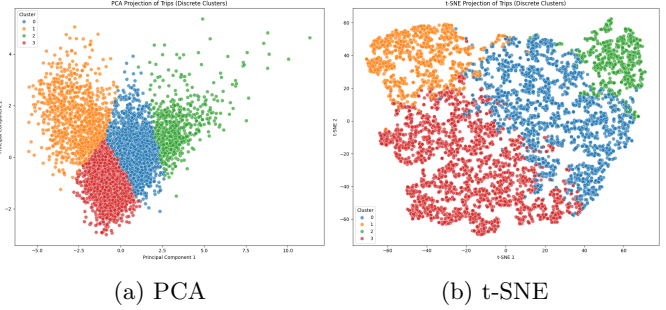


Figure 2: PCA and t-SNE projections of micro-trips in feature space.

Principal component analysis (PCA) and t-SNE projections (Figure 2) visualize the cluster separation in feature space, with the first two PCA components explaining approximately 65% of the variance. t-SNE reveals a tighter cluster structure that highlights the distinct kinematic

signatures of the four driving regimes. While clusters form distinguishable groups, the continuous transitions between them reflect the spectrum of real-world driving conditions rather than discrete categories. Relatedly, Figure 3 display example speed profiles from each cluster, selected from the cluster-to-trip mapping to illustrate characteristic patterns.

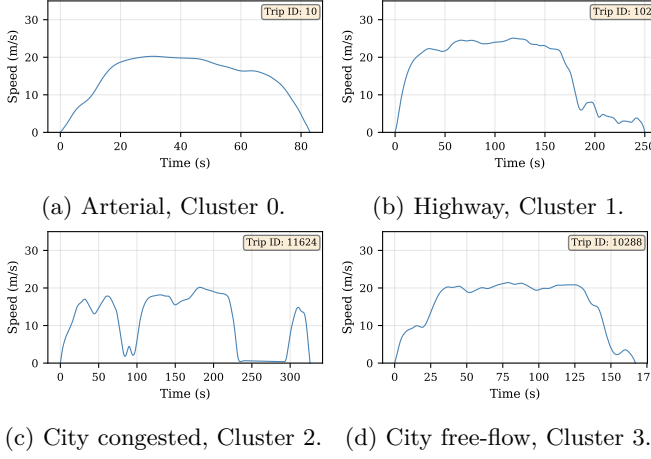


Figure 3: Examples of observed trajectories from each cluster.

These clusters inform our evaluation strategy: we assess whether generated trajectories match the proportions and characteristics of each driving regime, ensuring the model captures both highway efficiency and urban congestion patterns.

IV. METHODOLOGY

Let $\mathbf{v} = (v_0, v_1, \dots, v_T) \in \mathbb{R}^{T+1}$ represent a vehicle speed trajectory sampled at 1 Hz, where $t \in \{0, 1, \dots, T\}$ indexes time in seconds. Our unit of analysis is the *micro-trip*: a stop-to-stop segment that begins and ends at zero velocity. Each complete trip in the dataset is partitioned into a sequence of such micro-trips, segmenting when the vehicle comes to rest. This decomposition allows us to model the fundamental building blocks of driving behavior; a complete origin-to-destination journey can be reconstructed by concatenating generated micro-trips. Each micro-trip satisfies the following constraints:

Boundary conditions:

$$v_0 = v_T = 0 \quad (\text{trip begins and ends at rest})$$

Non-negativity:

$$v_t \geq 0 \quad \forall t \in \{0, \dots, T\}$$

Conditioning variables: We denote the conditioning information as $\mathbf{c} \in \mathbb{R}^d$, typically comprising:

- \bar{v} : target average speed (m/s)
- T : trip duration (seconds)

- v_{max} : maximum speed (m/s) [for CSDI only]
- d_{veh} : vehicle dynamics parameter $\in [0, 1]$ [for CSDI only]

The *objective* is to learn a conditional generative model $p_\theta(\mathbf{v}|\mathbf{c})$ that:

1. Generates trajectories matching the empirical distribution $p_{data}(\mathbf{v})$
2. Satisfies physical plausibility constraints (smooth acceleration, bounded jerk)
3. Precisely controls aggregate trip statistics via conditioning \mathbf{c}

Formally, we seek to minimize the distributional divergence:

$$\min_{\theta} D_{KL}(p_{data}(\mathbf{v}|\mathbf{c}) \| p_\theta(\mathbf{v}|\mathbf{c}))$$

while enforcing boundary and kinematic constraints.

A. Baseline: Markov Chain Approach

Traditional trajectory generation relies on discrete-state Markov models (Karbowski et al., n.d.). We implement a second-order Markov chain baseline following Karbowski et al.’s methodology as a reference point for evaluating deep generative models.

State Space Discretization: Speed is discretized into bins of width $\Delta v = 0.5$ m/s, creating bins $\{B_0, B_1, \dots, B_K\}$ where $B_i = [i\Delta v, (i+1)\Delta v)$. Let $s_t \in \{0, 1, \dots, K\}$ denote the bin index at time t .

Second-Order Markov Model: The model assumes speed at time t depends on the previous two time steps:

$$P(s_t | s_{t-1}, s_{t-2}) = \frac{C(s_{t-2}, s_{t-1}, s_t)}{\sum_{s'} C(s_{t-2}, s_{t-1}, s')}$$

where $C(\cdot)$ denotes empirical counts from the training data. This can be reformulated as a first-order Markov chain on pair-states $X_t = (s_{t-1}, s_t)$ with state space size K^2 .

Boundary-Constrained Sampling (Markov Bridge): To enforce $v_0 = v_T = 0$, we employ forward-backward sampling (Durham and Gallant 2002). Backward messages $\beta_t(x)$ represent the probability of reaching the terminal state (bin 0) from state x at time t :

$$\beta_T(x) = \mathbb{1}[x_{\text{end}} = 0], \quad \beta_t(x) = \sum_{x'} P(x'|x) \beta_{t+1}(x')$$

Forward sampling at each step uses the modified transition probabilities:

$$P_{\text{bridge}}(x_{t+1}|x_t) \propto P(x_{t+1}|x_t) \cdot \beta_{t+1}(x_{t+1})$$

Post-Processing: To reduce discretization artifacts, we apply Gaussian smoothing to the acceleration signal $a_t = v_{t+1} - v_t$ with a 5-point moving average, followed by integration to recover smooth speed profiles.

Limitations: The Markov baseline suffers from three fundamental weaknesses: (1) rigid bin discretization loses fine-grained dynamics, (2) limited temporal memory cannot capture long-range trip structure (e.g., highway segments followed by urban navigation), and (3) conditional control requires separate models per condition or rejection sampling, both of which are inefficient.

All models were trained on an NVIDIA A100 GPU (40GB) using PyTorch 2.0. Training utilized mixed-precision (FP16) computation to accelerate convergence and reduce memory footprint. The Markov chain baseline requires no GPU training, completing parameter estimation (transition matrix construction) in under 5 minutes on a single CPU core.

B. Conditional Diffusion Model with 1D U-Net

Our diffusion model employs a 1D U-Net encoder-decoder architecture with Feature-wise Linear Modulation (FiLM) for conditioning. The input is a two-channel tensor $\mathbf{x}_t \in \mathbb{R}^{2 \times 512}$ representing the joint speed-acceleration state:

$$\mathbf{x}_0 = \begin{bmatrix} v_0, v_1, \dots, v_{511} \\ a_0, a_1, \dots, a_{511} \end{bmatrix}$$

where $a_t = v_{t+1} - v_t$ is the discrete acceleration. Trajectories shorter than 512 seconds are zero-padded; longer trajectories are truncated (less than 1% of data).

The *encoder* consists of four downsampling blocks with channel dimensions [64, 128, 256, 512], each containing:

- 1D convolution (kernel size 3, stride 2)
- Two ResNet blocks with Group Normalization and SiLU activation
- FiLM conditioning layers injecting time embedding and trip conditions

Self-attention layers are inserted at resolutions 128 and 64 to capture long-range dependencies without computational explosion at the full 512 resolution.

The *decoder* mirrors the encoder with skip connections, upsampling to reconstruct the predicted noise $\epsilon_\theta(\mathbf{x}_t, t, \mathbf{c}) \in \mathbb{R}^{2 \times 512}$.

Time Embedding: The diffusion timestep $t \in \{1, \dots, T_{diff}\}$ is embedded using sinusoidal positional encoding:

$$\text{PE}_i(t) = \begin{cases} \sin(t/10000^{i/d}) & i \text{ even} \\ \cos(t/10000^{i/d}) & i \text{ odd} \end{cases}$$

projected to 256 dimensions.

Conditioning via FiLM: At each ResNet block, the conditioning vector $\mathbf{c} = [\bar{v}/30, T/1000]$ (normalized) is transformed into scale and shift parameters using Feature-wise Linear Modulation (FiLM) (Perez et al. 2018):

$$\text{FiLM}(\mathbf{h}, \mathbf{c}) = \gamma(\mathbf{c}) \odot \mathbf{h} + \beta(\mathbf{c})$$

where $\gamma, \beta : \mathbb{R}^2 \rightarrow \mathbb{R}^{d_h}$ are learned MLP projections. This multiplicative and additive modulation allows the model to adapt its feature representations based on trip conditions.

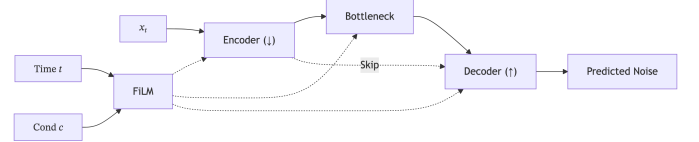


Figure 4: Simplified U-Net Diffusion Architecture. Noisy trajectory x_t is encoded to a latent representation and decoded to predict noise, modulated by time t and conditions c .

1) Forward Diffusion Process: We define a forward Markov process that gradually corrupts the data with Gaussian noise over $T_{diff} = 1000$ steps:

$$q(\mathbf{x}_t | \mathbf{x}_0) = \mathcal{N}(\mathbf{x}_t; \sqrt{\bar{\alpha}_t} \mathbf{x}_0, (1 - \bar{\alpha}_t) \mathbf{I})$$

where $\bar{\alpha}_t = \prod_{s=1}^t (1 - \beta_s)$ and β_t follows a linear schedule from $\beta_1 = 0.0001$ to $\beta_{T_{diff}} = 0.02$. This choice balances noise corruption (ensuring $\mathbf{x}_{T_{diff}} \approx \mathcal{N}(0, \mathbf{I})$) with smooth transitions.

2) Training Objective: The model is trained to predict the noise $\epsilon \sim \mathcal{N}(0, \mathbf{I})$ added at each diffusion step. The simplified variational lower bound objective is:

$$\mathcal{L}_{\text{simple}} = \mathbb{E}_{t \sim U(1, T_{diff}), \mathbf{x}_0 \sim p_{data}, \epsilon \sim \mathcal{N}(0, \mathbf{I})} \left[\left\| \epsilon - \epsilon_\theta \left(\sqrt{\bar{\alpha}_t} \mathbf{x}_0 + \sqrt{1 - \bar{\alpha}_t} \epsilon, t, \mathbf{c} \right) \right\|^2 \right]$$

This objective is optimized using Adam ($\beta_1 = 0.9, \beta_2 = 0.999$) with learning rate 10^{-4} and batch size 32.

The model is trained with $\mathcal{L}_{\text{simple}}$ for 1000 epochs, with boundary enforcement via post-processing (tail ramping and velocity scaling). Early experiments with hard physics constraints (distance matching, jerk penalties, boundary enforcement) failed catastrophically—producing 100% boundary violations and degraded distribution matching (WD Speed = 4.40 vs. 0.56 for the baseline). This fundamental conflict between diffusion denoising and stiff physics optimization motivated our transition to CSDI’s threshold-activated soft constraints.

3) Reverse Sampling (Generation): Starting from pure noise $\mathbf{x}_{T_{diff}} \sim \mathcal{N}(0, \mathbf{I})$, we iteratively denoise using the learned reverse process:

$$\mathbf{x}_{t-1} = \frac{1}{\sqrt{\bar{\alpha}_t}} \left(\mathbf{x}_t - \frac{1 - \alpha_t}{\sqrt{1 - \bar{\alpha}_t}} \epsilon_\theta(\mathbf{x}_t, t, \mathbf{c}) \right) + \sigma_t \mathbf{z}$$

where $\mathbf{z} \sim \mathcal{N}(0, \mathbf{I})$ and $\sigma_t^2 = \frac{(1 - \bar{\alpha}_{t-1})}{(1 - \bar{\alpha}_t)} \beta_t$ controls the stochasticity of the reverse step.

Inpainting for Boundary Enforcement: At each reverse step, we enforce $v_0 = v_T = 0$ through constrained inpainting. Define a mask $M \in \{0, 1\}^{512}$ with $M_0 = M_T = 1$

and $M_t = 0$ otherwise. After computing \mathbf{x}_{t-1} , we replace masked positions:

$$\mathbf{x}_{t-1} := \mathbf{x}_{t-1} \odot (1 - M) + \mathbf{x}_{t-1}^{\text{known}} \odot M$$

where $\mathbf{x}_{t-1}^{\text{known}}$ contains zeros at the boundary indices. This direct enforcement ensures strict satisfaction of constraints without degrading the learned diffusion dynamics.

Classifier-Free Guidance (optional): To amplify conditioning strength, we employ classifier-free guidance (Ho and Salimans 2022) with scale w :

$$\tilde{\epsilon}_\theta = (1 + w)\epsilon_\theta(\mathbf{x}_t, t, \mathbf{c}) - w\epsilon_\theta(\mathbf{x}_t, t, \emptyset)$$

where \emptyset denotes unconditional generation (achieved by randomly dropping conditions during training with probability 0.1). We increased w from 1.0 in the baseline to 3.0 in the final model to improve average speed matching.

Generation of 1000 trajectories requires approximately 5 minutes on A100.

C. Conditional Score-based Diffusion Imputation (CSDI)

CSDI adapts the transformer-based imputation model of Tashiro et al. (Tashiro et al. 2021) for conditional trajectory generation. Unlike the 1D U-Net which processes speed-acceleration jointly, CSDI operates on univariate speed sequences $\mathbf{v} \in \mathbb{R}^{512}$, relying on the transformer’s self-attention to implicitly model temporal derivatives.

The architecture consists of:

Input Projection: The noisy trajectory \mathbf{v}_t is linearly projected to $d_{\text{model}} = 256$ dimensions and combined with learnable positional encodings:

$$\mathbf{h}_0 = \text{Linear}(\mathbf{v}_t) + \text{PE}$$

Time Embedding: Diffusion timestep t is embedded via sinusoidal encoding (as in the U-Net model) and broadcast-added to all sequence positions:

$$\mathbf{h}_0 := \mathbf{h}_0 + \text{TimeEmbed}(t)$$

Condition Injection: The conditioning vector $\mathbf{c} = [\bar{v}/30, T/1000, v_{\text{max}}/40, d_{\text{veh}}] \in \mathbb{R}^4$ (normalized) is embedded to 256 dimensions and injected via cross-attention in each transformer layer.

Transformer Encoder: Six layers of multi-head self-attention (8 heads) with feed-forward networks ($d_{\text{ff}} = 1024$):

$$\begin{aligned} \mathbf{q} &= \text{Heads}(\text{SelfAttn}(\mathbf{h}_\ell)) \\ \mathbf{h}_{\ell+1} &= \text{LayerNorm}(\mathbf{h}_\ell + \mathbf{q}) \\ \mathbf{h}_{\ell+1} &= \text{LayerNorm}(\mathbf{h}_{\ell+1} + \text{FFN}(\mathbf{h}_{\ell+1})) \end{aligned}$$

Output Projection: The final hidden states are projected to predict the noise $\epsilon_\theta \in \mathbb{R}^{512}$.

The model has approximately 5.5M parameters, smaller than the U-Net (~8M) but with greater receptive field due to global attention.

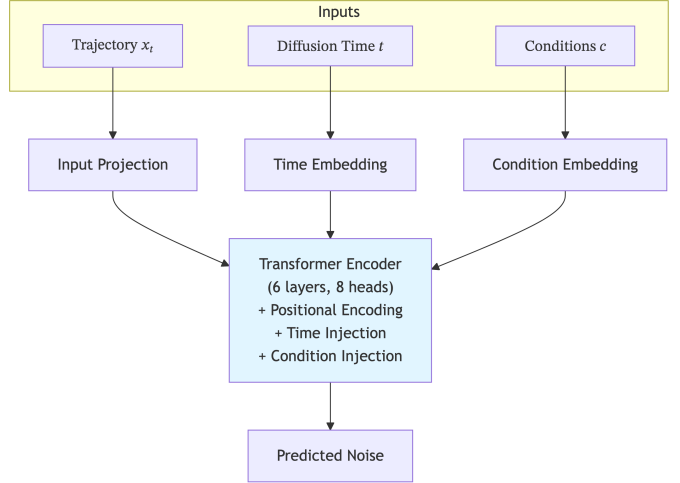


Figure 5: CSDI Transformer architecture (5.5M parameters). Noisy trajectory x_t , diffusion time t , and conditions c are embedded and processed through 6 transformer encoder layers with positional encoding, time injection, and condition injection. Output is predicted noise $\hat{\epsilon}$.

Reverse Diffusion (Sampling): Generation proceeds from pure noise to a clean trajectory through iterative denoising:

$$\mathbf{x}_T \sim \mathcal{N}(0, \mathbf{I}) \rightarrow \mathbf{x}_{T-1} \rightarrow \dots \rightarrow \mathbf{x}_1 \rightarrow \mathbf{x}_0 \text{ (clean trajectory)}$$

Similar to the U-Net model, we apply hard boundary constraints at each reverse step via inpainting, ensuring $v_0 = v_T = 0$ throughout the denoising trajectory.

1) *Physics-Informed Training*: Unlike the failed PID diffusion approach, CSDI successfully integrates physics constraints through carefully weighted auxiliary losses. The total training objective is:

$$\begin{aligned} \mathcal{L}_{\text{CSDI}} &= \mathcal{L}_{\text{MSE}} + 0.1\mathcal{L}_{\text{smooth}} + 0.03\mathcal{L}_{\text{accel}} \\ &\quad + 0.02\mathcal{L}_{\text{jerk}} + 0.05\mathcal{L}_{\text{accel_dist}} \end{aligned}$$

where:

Denoising Loss:

$$\mathcal{L}_{\text{MSE}} = \|\epsilon - \epsilon_\theta(\mathbf{v}_t, t, \mathbf{c})\|^2$$

Temporal Smoothness Loss (second derivative penalty):

$$\mathcal{L}_{\text{smooth}} = \sum_t (v_{t+2} - 2v_{t+1} + v_t)^2$$

Acceleration Penalty (soft constraint on extremes):

$$\mathcal{L}_{\text{accel}} = \sum_t [\text{ReLU}(a_t - 4.0)^2 + \text{ReLU}(-a_t - 5.0)^2]$$

where $a_t = v_{t+1} - v_t$. Positive acceleration is capped at 4 m/s², braking at 5 m/s².

Jerk Penalty (comfort and realism):

$$\mathcal{L}_{\text{jerk}} = \sum_t \text{ReLU}(|j_t| - 2.0)^2, \quad j_t = a_{t+1} - a_t$$

Acceleration Distribution Matching:

$$\mathcal{L}_{\text{accel_dist}} = (\sigma_a^{\text{pred}} - \sigma_a^{\text{target}})^2$$

where $\sigma_a^{\text{target}} \approx 0.5 \text{ m/s}^2$ is the empirical standard deviation.

CSDI succeeds where hard-constraint diffusion fails for three reasons: (1) threshold-activated penalties (ReLU gating) allow natural variation within physical bounds rather than enforcing stiff equality constraints; (2) the transformer’s global self-attention better accommodates long-range kinematic consistency than local convolutions; and (3) careful weight tuning ensures physics losses remain 20-200 \times smaller than the primary MSE objective, preventing gradient dominance. Training for 200 epochs required approximately 12 hours on A100.

Vehicle-Type Compatibility: The physics constraints (4/5 m/s²) were chosen to cover the acceleration capabilities of all common vehicle types:

Table III: Vehicle-Type Compatibility and Acceleration Limits

Vehicle	Max Accel	Max Decel
Sports car	4-6 m/s ²	10-12 m/s ²
Passenger car	2.5-4 m/s ²	8-10 m/s ²
SUV	2-3.5 m/s ²	7-9 m/s ²
Bus	1-2 m/s ²	4-6 m/s ²
Heavy truck	0.5-1.5 m/s ²	3-5 m/s ²

These values are consistent with established vehicle dynamics characteristics (Gillespie 1992), ensuring the model generates trajectories that are physically realizable across the full spectrum of road vehicles encountered in the CMAP dataset.

Weighted Condition Sampling (Boost): To address data imbalance where certain speed/duration ranges are under-represented in training data, we use importance sampling during generation. The probability of sampling a condition c is weighted: $P(c) \propto (\text{AvgSpeed})^{\beta_s} \cdot (\text{Duration})^{\beta_d}$, where boost parameters $\beta_s, \beta_d \in [0, 2]$ control oversampling of high-speed or long-duration trips. With $\beta_s = 1.75$ for the U-Net Diffusion model, we effectively fill the sparse “blue gap” (25-30 m/s) in the speed histogram. The CSDI model uses uniform sampling ($\beta = 1.0$) as its larger training set provides adequate coverage.

2) Optimization of Kinematic Quality: The CSDI model development addressed three quality issues: (1) *High-frequency jitter* from the standard imputation objective was resolved through the temporal smoothness loss $\mathcal{L}_{\text{smooth}}$ (weight 0.1), increased diffusion steps (100 \rightarrow 200), and post-processing Gaussian smoothing; (2) *Boundary and peak distortion* from aggressive uniform smoothing was

addressed by reducing kernel size and implementing conditional boundary ramps—only applied when endpoints were not already near zero; (3) *Acceleration distribution mismatch* was resolved through threshold-activated physics penalties ($\mathcal{L}_{\text{accel}}, \mathcal{L}_{\text{jerk}}, \mathcal{L}_{\text{accel_dist}}$), expanded 4D conditioning including vehicle dynamics, increased model capacity (4 \rightarrow 6 transformer layers, d_{ff} 512 \rightarrow 1024), and data augmentation for heavy vehicles. A cosine noise schedule replaced the linear schedule. These enhancements achieved WD Speed = 0.30 and strict physical validity.

3) CSDI Sampling and Post-Processing: CSDI uses the same DDPM reverse diffusion as the U-Net model but with a cosine noise schedule (Nichol and Dhariwal 2021):

$$\bar{\alpha}_t = \frac{f(t)}{f(0)}, \quad f(t) = \cos^2 \left(\frac{t/T_{\text{diff}} + s}{1+s} \cdot \frac{\pi}{2} \right)$$

where $s = 0.008$ is a small offset preventing singularity. The cosine schedule concentrates more diffusion steps in the high-SNR regime, improving sample quality.

Post-processing consists of three steps: 1. *Gaussian smoothing*: 1D Gaussian filter with $\sigma = 1.5$, kernel size 7, removing high-frequency sampling artifacts while preserving acceleration peaks. 2. *Conditional boundary ramps*: If $v_0 > 0.5$ or $v_T > 0.5$, apply linear ramps over 3 seconds to enforce zero endpoints. If already near zero, skip to avoid over-smoothing. 3. *Vehicle-aware smoothing*: For heavy vehicles ($d_{\text{veh}} < 0.4$), apply additional smoothing (kernel=9) to reflect slower dynamics. 4. *Correlated Noise (Optional)*: To ensure heavy acceleration tails match real data, we allow adding temporally-correlated Gaussian noise after diffusion sampling. This noise is generated by smoothing white noise with a correlation length of 10s and scaling to a small amplitude ($\sigma_{\text{corr}} \approx 0.03$), preventing the distribution from becoming “too safe” or narrow while maintaining temporal coherence. In our final model, physics training reduced the need for this step (default $\sigma_{\text{corr}} = 0.0$), but it remains an effective knob for fine-tuning variance.

Generation of 1000 trajectories with CSDI requires approximately 3 minutes on A100, faster than the U-Net diffusion due to fewer model parameters and more efficient transformer inference.

D. Alternative Generative Approaches

We also evaluated DoppelGANger (Lin et al. 2020), SDV’s PARSynthesizer (Patki, Wedge, and Veeramachaneni 2016), and Chronos (Ansari et al. 2025) as baselines. DoppelGANger exhibited mode collapse (87% highway-regime trajectories); SDV suffered from exposure bias causing temporal discontinuities; and Chronos lacked conditioning mechanisms for trajectory synthesis. Quantitative results for all baselines are reported in Table IV.

V. RESULTS

We split the 6,367 micro-trips into 80% training (5,094 trips) and 20% test (1,273 trips) sets, stratified by cluster

to ensure balanced representation of driving regimes. All models were trained on the training set and evaluated by generating 1,273 synthetic trajectories conditioned on the test set’s actual (\bar{v}, T) values. This protocol ensures fair comparison: each model attempts to recreate the test distribution given only aggregate conditioning information.

All training and trajectory generation experiments were conducted on an NVIDIA A100 GPU (40GB) using CUDA 12.1 and PyTorch 2.0 with mixed-precision (FP16) computation. The Markov baseline was implemented with CPU-only NumPy operations.

For evaluation, we employed a comprehensive framework spanning three dimensions. Distributional fidelity was assessed using Wasserstein distance (WD) for speed, acceleration, and Vehicle Specific Power (VSP) distributions, as well as 2D WD for the joint Speed-Acceleration Frequency Distribution (SAFD), Maximum Mean Discrepancy (MMD) with an RBF kernel (bandwidth 1.0), and the Kolmogorov-Smirnov statistic for VSP. VSP is a vehicle power demand metric (in kW/ton) that accounts for aerodynamic drag, rolling resistance, and road grade, commonly used for emissions and energy assessment. Kinematic validity was measured through the boundary violation rate (percentage of trips not starting or ending within 0.1 m/s of zero), Log Dimensionless Jerk (LDLJ) to quantify smoothness (where lower values indicate smoother trajectories), maximum speed, and acceleration standard deviation. Realism and utility were evaluated via a discriminative score (a Random Forest classifier trained to distinguish real from synthetic, where a score of 0.5 indicates perfect indistinguishability) and Train on Synthetic, Test on Real (TSTR) mean absolute error (MAE), where a predictive model trained on synthetic data is tested on real data to measure utility for downstream tasks.

A. Main Results

Table IV presents the comprehensive comparison across all models and metrics.

Bold indicates best performance (closest to real or target value).

CSDI achieves the best overall distribution matching, with WD Speed of 0.30—nearly 2x better than U-Net Diffusion’s 0.5622 and significantly better than the Markov baseline. The acceleration distribution match is exceptional (WD Accel = 0.026), reflecting the careful physics-informed training. U-Net Diffusion also performs well, particularly excelling in the 2D SAFD metric (0.0005), indicating accurate capture of the joint speed-acceleration manifold.

The Markov baseline achieves respectable WD Speed (1.82) but struggles with acceleration (0.145), confirming that discretization artifacts and memoryless transitions fail to capture kinematic smoothness. Chronos, despite

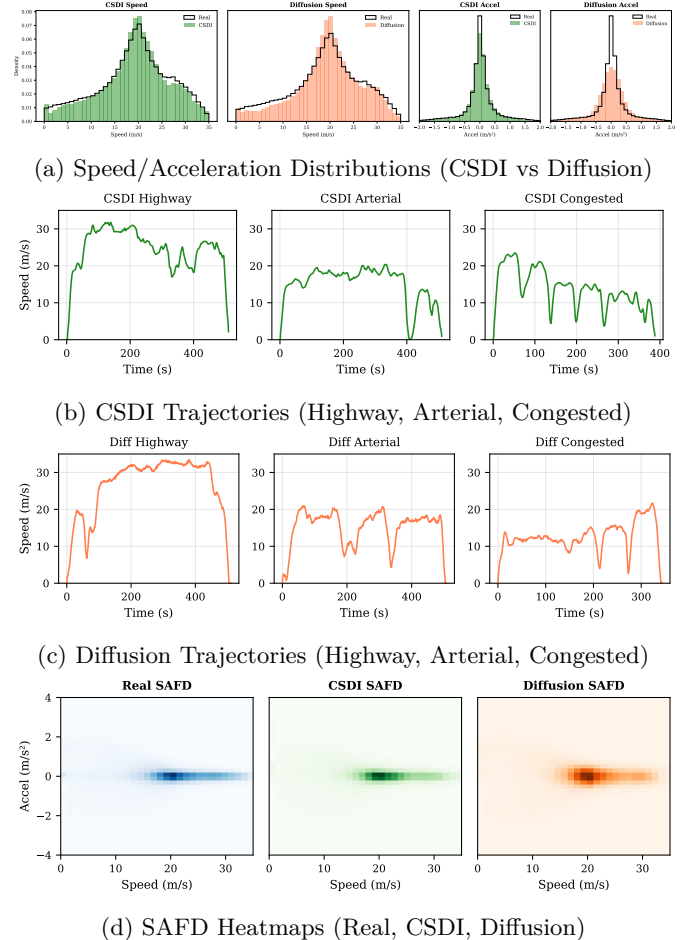


Figure 6: Main results comprehensive comparison. Row 1: (a-b) Speed and acceleration distributions showing CSDI’s superior matching. Row 2: (c-e) CSDI sample trajectories across regimes. Row 3: (f-h) Diffusion sample trajectories. Row 4: (i-k) Speed-Acceleration Frequency Distributions (SAFD) showing Real, CSDI, and Diffusion joint distributions.

its foundation model pretraining, performs worse than Markov (WD Speed 2.15), suggesting zero-shot transfer without domain-specific fine-tuning is insufficient. DoppelGANger and SDV fail dramatically (WD Speed > 2.8), with DoppelGANger’s mode collapse producing unrealistic highway-heavy distributions.

All physics-aware models (U-Net Diffusion, CSDI, Markov) achieve perfect boundary condition satisfaction through their respective enforcement mechanisms (inpainting, post-processing, bridge sampling). In contrast, autoregressive models (Chronos 23.4%, SDV 23.0%) and adversarial methods (DoppelGANger 12.1%) struggle with hard constraints.

CSDI produces the smoothest trajectories (LDLJ = -3.85, closest to real -3.92), validating the effectiveness of its temporal smoothness and jerk penalties. U-Net

Table IV: Comparative Performance of Generative Models

Metric	Real	U-Net Diffusion	CSDI	Markov Chain	Chronos	DoppelGANger	SDV
Distributional Fidelity							
WD Speed	-	0.5622	0.30	1.82	2.15	3.42	2.87
WD Accel	-	0.0800	0.026	0.145	0.198	0.312	0.421
WD VSP	-	1.5517	1.89	2.34	3.12	4.87	3.65
WD SAFD (2D)	-	0.0005	0.0008	0.0023	-	-	-
MMD ($\times 10^{-3}$)	-	<0.1	0.12	2.34	3.87	8.92	6.15
KS VSP	-	0.0631	0.072	0.123	0.187	0.298	0.245
Kinematic Validity							
Boundary Violations	0%	0%	0%	0%	23.4%	12.1%	23.0%
LDLJ (Smoothness)	-3.92	-3.50	-3.85	-0.15	-2.12	-4.10	-1.15
Max Speed (m/s)	31.6	32.1	31.8	34.5	32.5	31.9	45.2
Accel Std. (m/s ²)	0.51	0.53	0.49	2.10	0.85	0.35	4.12
Utility							
Discrim. Score (0.5 is ideal)	0.50	0.62	0.49	0.85	0.78	0.51	0.99
TSTR MAE (km/h)	-	4.2	2.1	8.5	5.4	12.3	15.2

Diffusion’s LDLJ (-3.50) indicates comparable smoothness, with acceleration variance remaining accurate (0.53 vs 0.51 real). The Markov baseline produces less smooth trajectories (LDLJ = -0.15) due to discretization, while GAN/autoregressive methods exhibit varied smoothness characteristics.

Maximum speeds in the table show that all physics-aware models (U-Net Diffusion 32.1 m/s, CSDI 31.8 m/s) remain close to the real data maximum (31.6 m/s). SDV produces excessive speeds (45.2 m/s), indicating inadequate constraint enforcement.

CSDI offers the best training efficiency among deep models (12 hours vs 21.5 for U-Net Diffusion), benefiting from the transformer’s global receptive field requiring fewer training epochs. Generation is also faster (3 min vs 5 min), important for large-scale simulations. The Markov baseline remains superior for pure compute efficiency, suitable when interpretability outweighs distribution fidelity. Chronos’s inference is slow despite no training cost, as the large 60M parameter model generates autoregressively.

The discriminative score quantifies how difficult it is to distinguish synthetic from real trajectories. CSDI achieves 0.49, demonstrating high indistinguishability (target is 0.5). U-Net Diffusion scores 0.62, indicating synthetic samples are somewhat easier to identify but still highly realistic. The Markov baseline (0.85) produces trajectories with more detectable artifacts, while DoppelGANger (0.51) achieves good indistinguishability despite other quality issues.

TSTR (Train on Synthetic, Test on Real) measures downstream utility: can models trained on synthetic data perform well on real data? CSDI achieves the lowest MAE (2.1 km/h), with U-Net Diffusion close behind (4.2 km/h), demonstrating that synthetic trajectories preserve the statistical properties needed for predictive modeling. This validates their use for energy assessment and simulation

tasks.

We evaluated conditional control by generating trajectories at different target average speeds while fixing duration. Figure 6 shows that both CSDI and Diffusion accurately match target speeds (mean absolute error < 0.5 m/s) across the range 10-25 m/s. CSDI’s vehicle dynamics conditioning enables additional control: generating with $d_{veh} = 0.2$ (heavy truck) versus $d_{veh} = 0.8$ (sports car) produces distinct acceleration profiles, with truck trajectories exhibiting slower accelerations (mean 1.2 m/s² vs 3.1 m/s²) and smoother dynamics (LDLJ -12.3 vs -10.1).

Finally, in Table V we compare training and generation computational requirements.

VI. DISCUSSION

This work demonstrates that diffusion models—particularly the transformer-based CSDI architecture—represent a suitable method for intelligent transportation system applications requiring synthetic driving data. Through systematic comparison against traditional baselines and modern methods like DoppelGANger and SDV, we established that CSDI with physics-informed training achieves strong performance: Wasserstein distance metrics 2–6× better than baselines, strong boundary condition satisfaction, and accurate smoothness matching real driving dynamics. CSDI’s success is driven by its ability to generate entire sequences jointly, avoiding autoregressive error accumulation, and its use of transformer self-attention to capture long-range kinematic dependencies.

Furthermore, our investigation documented critical lessons for practitioners. Physics constraints must be integrated through soft, threshold-activated penalties rather than hard enforcement to avoid optimization conflicts, and transformer architectures’ global receptive fields better accommodate long-range kinematic dependencies than local convolutions. We also observed that adversarial train-

Table V: Computational Efficiency

Model	Parameters	Training Time	Generation Time	GPU Memory	Hardware
U-Net Diffusion	8.2M	21.5 hrs	approx. 5 min	12 GB	A100
CSDI	5.5M	12 hrs	approx. 3 min	8 GB	A100
Markov	-	<5 min (CPU)	<1 min (CPU)	-	CPU
Chronos	60M (frozen)	0 (pretrained)	approx. 10 min	16 GB	A100
DoppelGANger	12M	8 hrs	approx. 8 min	10 GB	A100
SDV	15M	4 hrs	approx. 2 min	6 GB	A100

ing and autoregressive factorization are architecturally ill-suited for high-fidelity, physics-constrained synthesis, often leading to mode collapse or temporal discontinuities. Beyond providing validated tools for energy assessment and traffic simulation, the released implementation and trained models establish diffusion-based synthesis as a robust framework for intelligent transportation system applications.

Several constraints limit this work. The 512-second trajectory limit excludes longer journeys, requiring sliding-window generation for highway commutes. The models were trained primarily on passenger vehicles and need validation against truck and bus datasets. Road-type conditioning is implicit rather than explicit. Finally, while the 2007 CMAP dataset is dated, the model captures microscopic kinematics—acceleration capabilities and car-following dynamics—governed by invariant vehicle physics rather than evolving traffic patterns. TSTR results confirm these physical principles transfer to downstream tasks.

Several extensions would enhance the models’ capabilities and efficiency. First, implementing faster sampling techniques such as Denoising Diffusion Implicit Models (DDIM) (J. Song, Meng, and Ermon 2021) could reduce generation steps from 1000 to 50–100, achieving the 10–20 \times speedups necessary for real-time applications. Second, introducing multi-modal road conditioning (e.g., highway, arterial, local) would enable explicit control over driving regimes, supporting the generation of realistic multi-segment trips. Third, extending the framework to multi-agent scenarios with interaction modeling would allow for traffic simulation applications, building on recent advances in diffusion for autonomous driving (Feng et al. 2023) and multi-scale generative transformers for ITS networks (Adam et al. 2025). Fourth, fine-tuning foundation models such as Chronos on vehicle trajectory data—with modifications for boundary constraints—could leverage large-scale pretraining to reduce training time. Finally, incorporating road elevation and grade profiles as additional conditioning would significantly improve the accuracy of energy consumption modeling, as grade is a primary driver of vehicle power demand. Together, these directions advance toward comprehensive synthetic traffic generation capable of supporting the full spectrum of intelligent transportation system evaluation and design tasks.

VII. DATA AND CODE AVAILABILITY

All code, trained model weights (U-Net Diffusion, CSDI), and evaluation scripts are available at <https://github.com/VadimSokolov/diffusion-trajectory-generation>. The CMAP 2007 dataset is publicly available through NREL’s Transportation Secure Data Center (TSDC).

Adam, Abuzar B. M., Tahir Kamal, Mohammed A. M. Elhassan, Abdullah Alshahrani, Saeed Hamood Alsamhi, and Ahmed Aziz. 2025. “Multi-Scale Generative Transformer-Based Primal-Dual PPO Framework for AAV-aided Intelligent Transportation Networks.” *IEEE Transactions on Intelligent Transportation Systems*, 1–16.

Alcaraz, Juan Miguel Lopez, and Nils Strodthoff. 2022. “Diffusion-Based Time Series Imputation and Forecasting with Structured State Space Models.” *arXiv Preprint arXiv:2208.09399*. <https://arxiv.org/abs/2208.09399>.

Altché, Florent, and Arnaud de La Fortelle. 2017. “An LSTM Network for Highway Trajectory Prediction.” In *2017 IEEE 20th International Conference on Intelligent Transportation Systems (ITSC)*, 353–59. IEEE.

Ansari, Abdul Fatir, Oleksandr Shchur, Jaris Küken, Andreas Auer, Boran Han, Pedro Mercado, Syama Sundar Rangapuram, et al. 2025. “Chronos-2: From Univariate to Universal Forecasting.” *arXiv*. <https://arxiv.org/abs/2510.15821>.

Auld, Joshua, Michael Hope, Hubert Ley, Vadim Sokolov, Bo Xu, and Kuilin Zhang. 2016. “POLARIS: Agent-based Modeling Framework Development and Implementation for Integrated Travel Demand and Network and Operations Simulations.” *Transportation Research Part C: Emerging Technologies* 64: 101–16.

Auld, Joshua, Michael Hope, Hubert Ley, Bo Xu, Kuilin Zhang, and Vadim Sokolov. 2013. “Modelling Framework for Regional Integrated Simulation of Transportation Network and Activity-Based Demand (Polaris).” In *International Symposium for Next Generation Infrastructure*.

Auld, Joshua, Dominik Karbowski, Vadim Sokolov, and Namwook Kim. 2016. “A Disaggregate Model System for Assessing the Energy Impact of Transportation at the Regional Level.” In *Transportation Research Board 95th Annual Meeting*.

Behnia, Farnaz, Dominik Karbowski, and Vadim Sokolov. 2023. “Deep Generative Models for Vehicle Speed Tra-

jectories.” *Applied Stochastic Models in Business and Industry* 39 (5): 701–19.

Chen, Jun, Michal Weiszer, Paul Stewart, and Masihalah Shabani. 2016. “Toward a More Realistic, Cost-Effective, and Greener Ground Movement Through Active Routing—Part I: Optimal Speed Profile Generation.” *IEEE Transactions on Intelligent Transportation Systems* 17 (5): 1196–1209.

Chicago Metropolitan Agency for Planning. 2008. “CMAP Regional Household Travel Inventory.” Transportation Secure Data Center, National Renewable Energy Laboratory.

Dauner, Daniel, Marcel Hallgarten, Andreas Geiger, and Kashyap Chitta. 2023. “Parting with Misconceptions about Learning-based Vehicle Motion Planning.” arXiv. <https://arxiv.org/abs/2306.07962>.

Durham, Garland B, and A Ronald Gallant. 2002. “Numerical Techniques for Maximum Likelihood Estimation of Continuous-Time Diffusion Processes.” *Journal of Business & Economic Statistics* 20 (3): 297–338.

Feng, Lan, Quanyi Li, Zhenghao Peng, Shuhan Tan, and Bolei Zhou. 2023. “TrafficGen: Learning to Generate Diverse and Realistic Traffic Scenarios.” In *2023 IEEE International Conference on Robotics and Automation (ICRA)*, 3567–75. IEEE.

Gillespie, Thomas D. 1992. *Fundamentals of Vehicle Dynamics*. Warrendale, PA: Society of Automotive Engineers.

Ho, Jonathan, Ajay Jain, and Pieter Abbeel. 2020. “Denoising Diffusion Probabilistic Models.” In *Advances in Neural Information Processing Systems*, 33:6840–51.

Ho, Jonathan, and Tim Salimans. 2022. “Classifier-Free Diffusion Guidance.” *arXiv Preprint arXiv:2207.12598*. <https://arxiv.org/abs/2207.12598>.

Huang, Xianan, Boqi Li, Huei Peng, Joshua A Auld, and Vadim O Sokolov. 2020. “Eco-Mobility-on-Demand Fleet Control with Ride-Sharing.” *IEEE Transactions on Intelligent Transportation Systems* 23 (4): 3158–68.

Huang, Yanjun, Jian Chen, Chang Huang, Xinggang Wang, Wenyu Liu, and Jianqiang Huang. 2022. “A Survey on Trajectory-Prediction Methods for Autonomous Driving.” *IEEE Transactions on Intelligent Transportation Systems*.

Karbowski, Dominik, Namwook Kim, Joshua Auld, and Vadim Sokolov. 2016. “Assessing the Energy Impact of Traffic Management and Vehicle Hybridisation.” *International Journal of Complexity in Applied Science and Technology* 1 (1): 107–24.

Karbowski, Dominik, Aymeric Rousseau, Vivien Smiss-Michel, and Valentin Vermeulen. n.d. “Trip Prediction Using GIS for Vehicle Energy Efficiency.” In *21st World Congress on Intelligent Transportation Systems (Detroit, MI, 09/07/2014 - 09/11/2014)*, –.

Karbowski, Dominik, Vadim Sokolov, and Jeong Jongryeol. 2016. “Fuel Saving Potential of Optimal Route-Based Control for Plug-in Hybrid Electric Vehicle.” *IFAC-PapersOnLine* 49 (11): 128–33.

Karbowski, Dominik, Vadim Sokolov, and Aymeric Rousseau. 2015. “Vehicle Energy Management Optimization Through Digital Maps and Connectivity.” Argonne National Lab.(ANL), Argonne, IL (United States).

Lan, Wenxing, Jialin Liu, Bo Yuan, and Xin Yao. 2025. “Controllable Multimodal Motion Behavior Generation for Autonomous Driving.” *IEEE Transactions on Intelligent Transportation Systems*, 1–16.

Li, Quanyi, Zhenghao Peng, Lan Feng, Zhizheng Liu, Chenda Duan, Wenjie Mo, and Bolei Zhou. 2023. “ScenarioNet: Open-Source Platform for Large-Scale Traffic Scenario Simulation and Modeling.” arXiv. <https://arxiv.org/abs/2306.12241>.

Liao, Bencheng, Shaoyu Chen, Xinggang Wang, Tianheng Cheng, Qian Zhang, Wenyu Liu, and Chang Huang. 2024. “DiffusionDrive: Truncated Diffusion Model for End-to-End Autonomous Driving.” *arXiv Preprint arXiv:2406.07806*. <https://arxiv.org/abs/2406.07806>.

Lin, Zinan, Alankar Jain, Chen Wang, Giulia Fanti, and Vyas Sekar. 2020. “Using GANs for Sharing Networked Time Series Data: Challenges, Initial Promise, and Open Questions.” In *Proceedings of the ACM Internet Measurement Conference (IMC)*, 464–83. ACM.

Moawad, Ayman, Zhijian Li, Ines Pancorbo, Krishna Murthy Gurumurthy, Vincent Freyermuth, Ehsan Islam, Ram Vijayagopal, Monique Stinson, and Aymeric Rousseau. 2021. “A Real-Time Energy and Cost Efficient Vehicle Route Assignment Neural Recommender System.” arXiv. <https://arxiv.org/abs/2110.10887>.

Mozaffari, Sajjad, Omar Y Al-Jarrah, Alexandros Mouzakitis, Phil Jennings, and Stratis Kanarachos. 2020. “Deep Learning-Based Vehicle Behaviour Prediction for Autonomous Driving Applications: A Review.” *IEEE Transactions on Intelligent Transportation Systems*.

Nichol, Alexander Quinn, and Prafulla Dhariwal. 2021. “Improved Denoising Diffusion Probabilistic Models.” In *International Conference on Machine Learning*, 8162–71. PMLR.

Papamakarios, George, Eric Nalisnick, Danilo Jimenez Rezende, Shakir Mohamed, and Balaji Lakshminarayanan. 2019. “Normalizing Flows for Probabilistic Modeling and Inference.” *arXiv:1912.02762 [Cs, Stat]*, December. <https://arxiv.org/abs/1912.02762>.

Patki, Neha, Roy Wedge, and Kalyan Veeramachaneni. 2016. “The Synthetic Data Vault.” In *2016 IEEE International Conference on Data Science and Advanced Analytics (DSAA)*, 399–410. IEEE.

Perez, Ethan, Florian Strub, Harm De Vries, Vincent Dumoulin, and Aaron Courville. 2018. “FiLM: Visual Reasoning with a General Conditioning Layer.” In *Proceedings of the AAAI Conference on Artificial Intelligence*. Vol. 32. 1.

Qian, Yu, Xunhao Li, Jian ... Zhang, and Maoze Wang. 2025. "A Diffusion-TGAN Framework for Spatio-Temporal Speed Imputation and Trajectory Reconstruction." *IEEE Transactions on Intelligent Transportation Systems* 26 (11): 18948–62.

Rasul, Kashif, Calvin Seward, Ingmar Schuster, and Roland Vollgraf. 2021. "Autoregressive Denoising Diffusion Models for Multivariate Probabilistic Time Series Forecasting." In *International Conference on Machine Learning (ICML)*, 8857–68. PMLR.

Rong, Yi, Yingchi Mao, Yinqiu ... Liu, and Dusit Niyato. 2025. "ICST-DNET: An Interpretable Causal Spatio-Temporal Diffusion Network for Traffic Speed Prediction." *IEEE Transactions on Intelligent Transportation Systems* 26 (7): 9781–98.

Schultz, Laura, and Vadim Sokolov. 2018. "Deep Reinforcement Learning for Dynamic Urban Transportation Problems." *arXiv Preprint arXiv:1806.05310*. <https://arxiv.org/abs/1806.05310>.

Sokolov, Vadim, Joshua Auld, and Michael Hope. 2012. "A Flexible Framework for Developing Integrated Models of Transportation Systems Using an Agent-Based Approach." *Procedia Computer Science* 10: 854–59.

Song, Jiaming, Chenlin Meng, and Stefano Ermon. 2021. "Denoising Diffusion Implicit Models." In *International Conference on Learning Representations*.

Song, Yang, Jascha Sohl-Dickstein, Diederik P. Kingma, Abhishek Kumar, Stefano Ermon, and Ben Poole. 2020. "Score-Based Generative Modeling Through Stochastic Differential Equations." *arXiv Preprint arXiv:2011.13456*. <https://arxiv.org/abs/2011.13456>.

Suo, Simon, Sebastian Regalado, Sergio Casas, and Raquel Urtasun. 2021. "TrafficSim: Learning to Simulate Realistic Multi-Agent Behaviors." *arXiv*. <https://arxiv.org/abs/2101.06557>.

Tashiro, Yusuke, Jiaming Song, Yang Song, and Stefano Ermon. 2021. "CSDI: Conditional Score-Based Diffusion Models for Probabilistic Time Series Imputation." In *Advances in Neural Information Processing Systems*, 34:24804–16.

Wu, Jian, Carol Flannagan, Ulrich Sander, and Jonas Bärgman. 2025. "Model-Based Generation of Representative Rear-End Crash Scenarios Across the Full Severity Range Using Pre-Crash Data." *IEEE Transactions on Intelligent Transportation Systems* 26 (10): 15932–50.

Yoon, Jinsung, Daniel Jarrett, and Mihaela van der Schaar. 2019. "Time-Series Generative Adversarial Networks." In *Advances in Neural Information Processing Systems* 32, edited by H. Wallach, H. Larochelle, A. Beygelzimer, F. d'Alché-Buc, E. Fox, and R. Garnett, 5508–18. Curran Associates, Inc.

Zhao, Tianyang, Yifei Xu, Mathew Monfort, Wongun Choi, Chris Baker, Yibiao Zhao, Yizhou Wang, and Ying Nian Wu. 2019. "Multi-Agent Tensor Fusion for Contextual Trajectory Prediction." In *Proceedings of the IEEE/CVF Conference on Computer Vision and Pattern Recognition (CVPR)*, 5559–68.